DOI: 10.1002/cphc.201100638

Comparison between Two Anionic Reverse Micelle Interfaces: The Role of Water–Surfactant Interactions in Interfacial Properties

Silvina S. Quintana, R. Dario Falcone, Juana J. Silber, and N. Mariano Correa*[a]

The water/sodium bis(2-ethylhexyl) phosphate (NaDEHP) reverse micelle (RM) system is revisited by using, for the first time, molecular probes to investigate interface properties. The solvatochromic behavior of 1-methyl-8-oxyquinolinium betaine (QB) and 6-propionyl-2-(*N*,*N*-dimethyl)aminonaphthalene (PRODAN) in the water/NaDEHP/toluene system is studied, and the results are compared with those obtained in water/sodium 1,4-bis(2-ethylhexyl) sulfosuccinate (AOT)/toluene RM media. The results demonstrate that the micropolarity, microviscosity, interfacial water structure, molecular probe partition, and intramolecular electron-transfer processes are dramatically altered for NaDEHP RM interfaces in comparison to the AOT systems. Because of organic nonpolar solvent penetration into the interface, NaDEHP RM media offer an interface with lower micropolarity and microviscosity than AOT media. Also, the interfacial water in the NaDEHP system shows enhanced water–water hydrogen-bond interaction in comparison with bulk water. The AOT RM interface represents a unique environment for PRODAN to undergo dual emission.

1. Introduction

Reverse micelles (RMs), a spatially ordered macromolecular assembly of surfactant molecules randomly distributed in nonpolar media, are of considerable practical importance in detergency, foodstuffs, cosmetics, chemical and biological reactions, separation technology, and materials synthesis.[1,2] When surfactants assemble in RMs, their polar or charged groups are located in the interior (or core) of the aggregates, while their hydrocarbon tails extend into the bulk organic solvent. In view of its easy preparation, stability, and ability to solubilize a large amount of water, Aerosol-OT (AOT, sodium 1,4-bis(2-ethylhexyl) sulfosuccinate, Scheme 1) is the most widely used surfactant in the study of RMs. Water added to the AOT systems is entrapped in the polar core, thereby forming a water pool surrounded by a layer of surfactant molecules. AOT has the remarkable ability to solubilize a large amount of water with values of [water]/[AOT] (W_0) as large as 40 to 60 depending on the surrounding nonpolar medium, the solute, and the temperature. However, the droplet size depends only on the W_0 value. Moreover, the bulk properties of water (polarity, viscosity, hydrogen-bonding ability, etc.) inside the pool (free) or at the interface (bound) also change with the W_0 values.[3–7] The interfacial region is known to have high ionic strength and a heterogeneous micropolarity.[8]

The dialkyl phosphates and their alkaline salts are of interest in extraction processes because of their complexing properties toward metal ions and are important in hydrometallurgy, the nuclear industry, and biological materials.[9] Among them, sodium bis(2-ethylhexyl) phosphate (NaDEHP, Scheme 1) has the particular property to give rise to RMs in organic solvents, as first pointed out by Eicke and Christen.[10] NaDEHP is of particular interest for comparison with AOT because of its similar structure and also because it has a similar phosphate head group to that of phospholipids.

The static and dynamical properties of water/NaDEHP/benzene RMs have been investigated by using several techniques.[11] ^{1}H NMR spectroscopy, densimetry, as well as light and neutron scattering experiments show that the domains of stability of these micelles correspond to water/surfactant ratios $W_0 < 6$. Above $W_0 = 3.5$, the release of free water molecules and sodium ions in the micellar core is evidenced by ^{1}H and ^{23}Na NMR spectroscopy and corresponds to the onset of electrical conductivity. Also, they have found a mean aggregation number of 12 ± 1 for a critical micelle concentration (CMC) of 8×10^{-3} M. Additionally, the anisotropic motions of water and

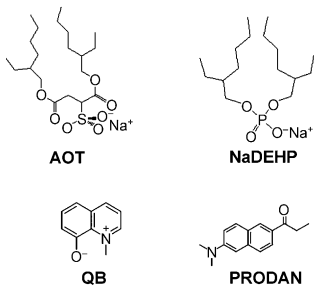

Scheme 1. Molecular structures of AOT, NaDEHP, QB, and PRODAN.

[a] *S. S. Quintana, Dr. R. D. Falcone, Prof. J. J. Silber, Prof. N. M. Correa*
Departamento de Química
Universidad Nacional de Río Cuarto
Agencia Postal #3, (X5804ALH) Río Cuarto (Argentina)
E-mail: mcorrea@exa.unrc.edu.ar

Supporting information for this article is available on the WWW under http://dx.doi.org/10.1002/cphc.201100638.

surfactant molecules were studied by multinuclear relaxation experiments.[11,12]

Neuman's group studied the micellization of NaDEHP in *n*-heptane[13] under controlled environmental conditions by using dynamic and static light scattering. The results clearly show that a trace amount of water has a very dramatic effect on reversed micellization. In contrast with results in the literature, water seemed to act as an antimicellization agent. Later studies showed that NaDEHP in *n*-heptane forms giant rodlike RMs[14,15] with a radius of gyration as large as 53 nm, which contrasted with the literature view, at that time, that the average micellar aggregation numbers in nonpolar media are much smaller (seldom exceeding 20) than those in aqueous media.

Very recently, similar results have been reported by molecular modeling.[16] Both geometry optimization and dynamic simulations indicate that NaDEHP aggregates that form in the organic phase are RMs. The main forces between the NaDEHP molecules are van der Waals and electrostatic forces.

On the other hand, Feng and Schelly[17] have proposed an alternative explanation for Newman's results and have challenged the water antimicellization idea. They have studied several properties of the water/NaDEHP/benzene system and the results suggest that below the "critical water content" ($W_0 \approx 3.0$) the aggregates are large rod-shaped dipolar crystallites with the same structure as the constituent rods of the hexagonal liquid-crystalline solid state of NaDEHP. At $W_0 > 3.0$ they have shown that the large aggregates successively dissolve and become spherical RMs, the sizes of which grow with the W_0 value. They have also shown that the sizes of the water/NaDEHP/benzene RMs are larger than those of the water/AOT/benzene RMs.

Li et al. performed a comparative study of water/NaDEHP/*n*-heptane and water/AOT/*n*-heptane by means of FTIR[18–20] and ^{1}H NMR spectroscopy,[19,20] and electrical conductimetry.[20] The ^{1}H NMR water signal shows a downfield shift in the water/AOT/*n*-heptane RMs, whereas it exhibits an upfield chemical shift in the NaDEHP system with an increase of the water content. The phenomenon of opposite tendency is also observed in the infrared spectra. As the W_0 values increase the O–H stretching bands of entrapped water shift from higher frequencies (than the bulk water value) for AOT RMs and from lower frequencies for NaDEHP RMs, toward the value of bulk water. The unusual spectroscopic behavior of solubilized water in the two systems was attributed to its strong interactions with surfactant ions and to the change in morphology and sizes of surfactant aggregates with increasing water content.

However, to the best of our knowledge, there are no studies using molecular probes to investigate valuable interface properties, such as micropolarity, microviscosity, solubilization power, molecular recognition, and intramolecular electron-transfer processes among others, in NaDEHP/aromatic solvent systems. Surprisingly these properties were unreported before in the literature.

In this work, we chose 1-methyl-8-oxyquinolinium betaine (QB) and 6-propionyl-2-(*N*,*N*-dimethyl)aminonaphthalene (PRODAN) as molecular probes because they are very sensitive to most of the RM interface properties named above.[21–25] QB is a molecular probe that has a UV/Vis absorption spectrum with two major features: a band in the visible region, B_1, that is primarily sensitive to polarity, and a band peaking at a shorter wavelength in the UV, B_2, which reflects the hydrogen-bond donor capability of the solvent.[21,22] The absorbance of the B_2 band is highly sensitive to the molecule's environment; hence the ratio of the absorbances of B_2 to B_1 ($AbsB_2/AbsB_1$), in combination with the absorption band shifts, provides an effective method to determine the properties of the microenvironment surrounding the probe.

On the other hand, PRODAN is widely used as a fluorescent molecular probe due to its significant Stokes shift in polar solvents. It is an aromatic compound with intramolecular charge-transfer (ICT) states, and can be particularly useful as a sensor for different kinds of media such as RMs and other membrane mimickers.[24–36] It is a fluorescent probe that exhibits strong shifts in the absorption and emission spectra on varying the environment. The probe emits an intense, single, broad fluorescence band, strongly red-shifted upon increasing the polarity–polarizability (π^*) and the hydrogen-donor ability (α) of the media.[32,37–39] We have demonstrated by using absorption and emission spectroscopies (stationary, time-resolved emission spectroscopy (TRES) and time-resolved area-normalized emission spectroscopy (TRANES)) that PRODAN in AOT reverse micellar media undergoes a partition process between the external nonpolar solvent and the RM interface. The molecular probe located in the nonpolar organic solvent always emits from a locally excited (LE) state whereas PRODAN located at the RM interface can emit from LE or ICT or both states (dual fluorescence) at room temperature depending on the AOT RM interface properties (see Scheme 2).[24,25] Furthermore, for PRODAN molecules located at the RM interfaces the results are consistent with the emission of the probe located in a single place within the AOT RM interface from two different excited states rather than from the emission of one excited state of the probe located in a different microenvironment: the interface and the water pool.[24,25] Moreover, we have shown the possibility of switching the state from where PRODAN emits by changing the properties of the AOT RM interfaces.[25] Adhikary et al.,[40] by solvation dynamics, have found that the LE and ICT states of PRODAN solvate on different timescales in AOT RMs (2 and ≈ 0.4 ns, respectively), consistent with our results. In consequence, the photophysics of PRODAN is very helpful to test the unique RM interface properties.[25]

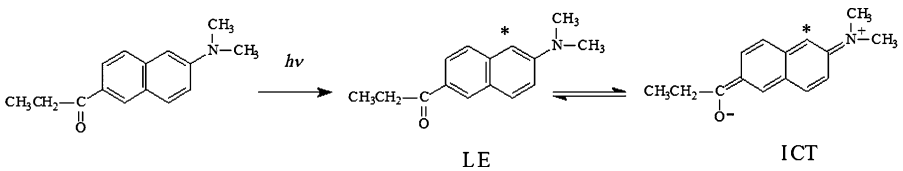

Scheme 2. Locally excited (LE) and intramolecular charge-transfer (ICT) structures of PRODAN.

Since the literature for NaDEHP and AOT RMs shows that the most common aromatic nonpolar organic solvent used is benzene, we measured the probe properties first in water/NaDEHP/benzene and water/AOT/benzene RMs. Afterwards, we changed benzene for toluene to try and use a more environmentally benign solvent. We found that there are no differences in the properties of the RMs and consequently we inform all the studies in water/NaDEHP/toluene and water/AOT/toluene RMs.

To evaluate differences in the unique interfacial properties of different RMs, we studied the solvatochromic behavior of QB and PRODAN in water/NaDEHP/toluene and water/AOT/toluene RMs by means of absorption and emission spectroscopy, at different surfactant and water concentrations. Our results show that, because of the aromatic solvent penetration, NaDEHP reverse micellar media offer an interface with lower micropolarity and microviscosity than AOT RMs. Also, the interfacial water inside NaDEHP RMs has the water–water hydrogen-bond interaction enhanced in comparison with bulk water. The differences were manifested when these RM interfaces were used to control from which excited state PRODAN can emit. The AOT RM interface represents a unique environment for PRODAN to undergo dual emission.

2. Results and Discussion

QB in Water/NaDEHP/Toluene RMs

Figure 1 and Figure 2 show the QB absorption spectra obtained by varying [NaDEHP] at [QB] = 2×10^{-4} M and $W_0 = 1$ and 10, respectively. We chose these W_0 values because it is known that NaDEHP RMs change their shape from ellipsoidal to spherical at a W_0 value around 3.[17] Thus, we wanted to investigate, at the molecular level, how the interfacial properties and the water–surfactant interactions are changed with the RM shape transition. Moreover, the feature for the QB spectra with varying W_0 values ([NaDEHP] = constant) is similar to the spectra found in AOT RMs,[21] and thus we do not show these spectra.

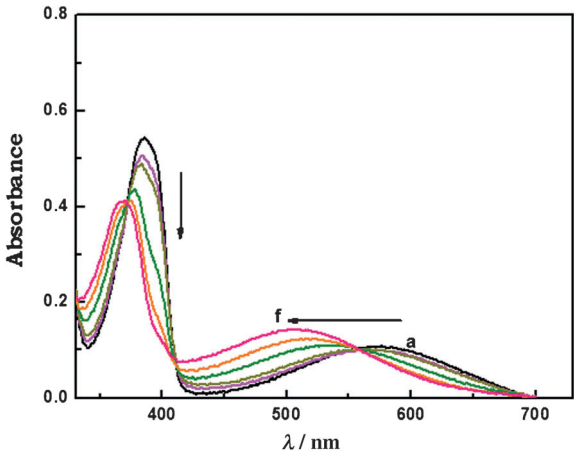

Figure 1. QB absorption spectra in water/NaDEHP/toluene RMs as a function of [NaDEHP] at $W_0 = 1$. [NaDEHP]: a) 0, b) 2.5×10^{-5}, c) 1×10^{-4}, d) 2.5×10^{-3}, e) 5×10^{-2}, f) 0.1 M. [QB] = 2×10^{-4} M.

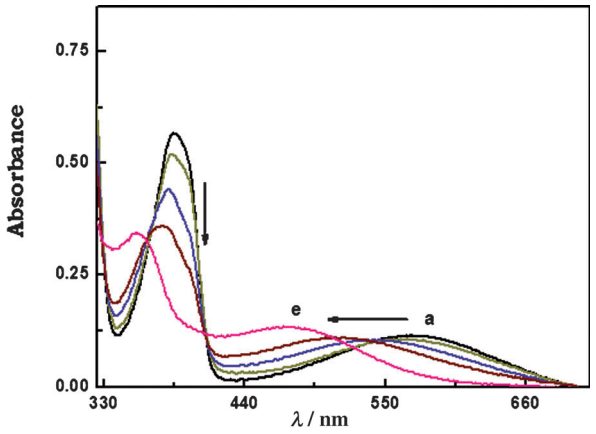

Figure 2. QB absorption spectra in water/NaDEHP/toluene RMs as a function of [NaDEHP] at $W_0 = 10$. [NaDEHP]: a) 0, b) 2.5×10^{-5}, c) 1×10^{-4}, d) 2.5×10^{-2}, e) 0.1 M. [QB] = 2×10^{-4} M.

As can be seen, there are hypsochromic shifts of the B_1 and B_2 bands. Interestingly, while the intensity of the B_1 band remains practically constant, the intensity of the B_2 band decreases as the surfactant concentration increases. The neat isosbestic point at $\lambda = 555$ nm detected at $W_0 = 1$ (Figure 1) suggests that an equilibrium between free QB in toluene and QB bound to the micelle interface is established.[41–45] On the other hand, Figure 2 shows that this equilibrium is absent when the water content is equal to 10. Similar results were obtained for AOT RMs at this W_0 value.[22]

Figure 3a and b summarize the λ_{max} B_1 and the $AbsB_2/AbsB_1$ ratio values for QB in water/NaDEHP/toluene RMs, respectively, upon varying [NaDEHP] at $W_0 = 1$ and 10. As can be observed there are changes in the polarity and the hydrogen-bond donor ability of the media[21,22] as the surfactant concentration increases, which is more important at $W_0 = 10$. Additionally, a definite zone of surfactant concentration can be observed where the changes in the micropolarities are more noticeable (Figure 3a).

The solvatochromic behavior of QB shows important differences between AOT and NaDEHP RM interfaces. For water/NaDEHP/toluene media, the hypsochromic shift observed in the λ_{max} B_1 values (Figure 1, Figure 2, and Figure 3a) is consistent with the increases in micropolarity as QB is incorporated into the RM interface. As expected, the changes are more significant in the presence of water ($W_0 = 10$).[21,22] Similar results were obtained previously for AOT RMs.[21] From the inflection point of the plot presented in Figure 3a, the CMCs at both W_0 values were determined and the results are reported in Table 1. Since it is known that for RM media the CMC values depend on the method used for their determination, it is customary to define this concentration as the operational CMC.[22,23,45] The values found using QB were similar to other CMC values obtained for water/NaDEHP/toluene systems using very different techniques.[11,17] Comparing the CMC values for NaDEHP and AOT (Table 1) at the same W_0 value, it can be

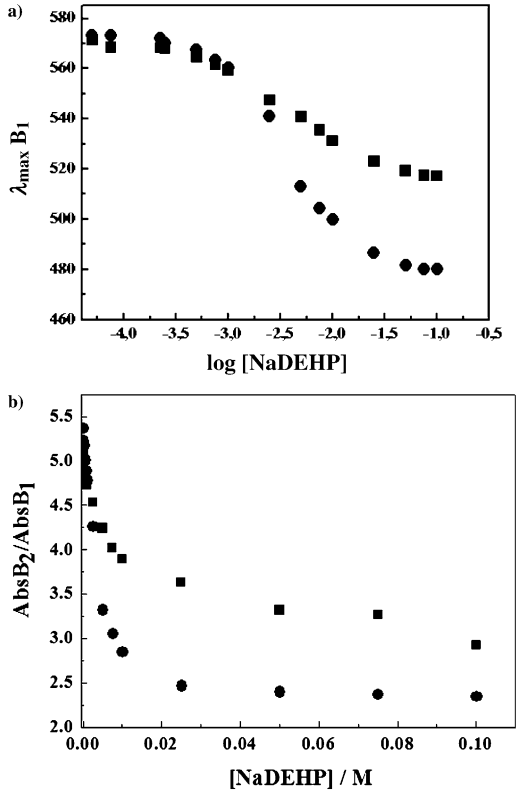

Figure 3. a) Variation of the B_1 band (λ_{max} B_1) in water/NaDEHP/toluene as a function of log [NaDEHP] at $W_0 = 1$ (■) and 10 (●). [QB] = 2×10^{-4} M. b) Variation of $AbsB_2/AbsB_1$ in water/NaDEHP/toluene as a function of [NaDEHP] at $W_0 = 1$ and 10. [QB] = 2×10^{-4} M.

Table 1. B_1 maximum absorption band and absorbance ratio ($AbsB_2/AbsB_1$) values of QB in AOT/toluene and NaDEHP/toluene RMs. [Surfactant] = 0.1 M.

Reverse micelles	$W_0 = 1$			$W_0 = 10$		
	λ_{max} B_1 [nm]	$AbsB_2/AbsB_1$	CMC [M]	λ_{max} B_1 [nm]	$AbsB_2/AbsB_1$	CMC [M]
NaDEHP/toluene	517	3.30	7×10^{-3}	474	2.36	3×10^{-3}
AOT/toluene	497	2.84	3×10^{-3}	465	2.00	4×10^{-4}

seen that the CMC is lower for AOT than for NaDEHP RMs. The result shows that the surfactant aggregation process is favored with AOT at both W_0 values, probably reflecting the fact that in NaDEHP experiments a shape transition occurs at W_0 around 3.[17] As was previously demonstrated for AOT,[22] in both RMs the presence of water helps RM formation with consequent decreases in the CMC value.

Nevertheless, a question may arise here about where QB is located in both RMs. To know the proper location of the probe is crucial to infer RM properties. We have to consider that QB is soluble in toluene and can undergo a partition process between the two different pseudophases: the RM interface and the nonpolar organic solvent. Figure 2 shows that there is no isosbestic point for QB spectra in NaDEHP/toluene RMs at $W_0 = 10$, and the same trend is observed for AOT/benzene RMs.[22] This suggests that when the amount of water is high enough to solvate the RM interface, QB is anchored to the interface through hydrogen-bond interaction with the interfacial water. Under these conditions the partition process between the two pseudophases is negligible. Moreover, the significant diminishing in the $AbsB_2/AbsB_1$ values shown in Figure 3b is consistent with a dramatic increase in the hydrogen-bond donor ability of the medium upon NaDEHP RM formation, similar to what was found for AOT RMs.[22] Thus, as in the case of AOT RMs, it seems that hydrogen bonding is the main interaction between water and the NaDEHP polar head group.

On the other hand, for NaDEHP/toluene and AOT/toluene RMs at $W_0 = 1$, where isosbestic points are detected in the QB absorption spectra (Figure 1), a partition constant was calculated from the spectral changes with the surfactant concentration (see the Supporting Information) and the K_p values obtained are gathered in Table S1 (Supporting Information). As can be seen, the K_p values are large enough to assure that at [surfactant] = 0.1 M more than 95% of QB exists at the interface. Thus, QB will monitor the changes in the interface properties at high surfactant concentration, as was observed for QB in different RMs.[21,22,46]

Thus, to monitor the RM interfacial properties we decided to work at [NaDEHP] or [AOT] = 0.1 M. In Table 1 are gathered the values of λ_{max} B_1 and $AbsB_2/AbsB_1$ ratio for QB in water/NaDEHP/toluene at [NaDEHP] = 0.1 M at $W_0 = 1$ and 10. The spectroscopic parameter values for QB in water/AOT/toluene RMs at $W_0 = 1$ and 10 are shown in Table 1 for comparison.

By analyzing the QB λ_{max} B_1 data gathered in Table 1 it can be seen that the micropolarity of the RM interface is higher for AOT/toluene than NaDEHP/toluene at any W_0 value studied. The lower micropolarity of the NaDEHP/toluene interface sensed by QB may be attributed to the aromatic solvent penetration into the RM interface, as was previously observed by Faure et al. from NMR experiments.[12] Furthermore, this solvent penetration into the NaDEHP interfacial zone makes the interfacial water–phosphate interaction weaker than the interfacial water–sulfonate (AOT) interaction, as reflected in the high value of the $AbsB_2/AbsB_1$ ratio obtained for NaDEHP/toluene RMs at both W_0 values (Table 1). Also, the less rigid interface for NaDEHP RMs probably favors interdroplet interactions with consequent larger droplet sizes in comparison with AOT RMs, as reported before.[17] In this sense, the work of Feng and Schelly[17] shows that the NaDEHP RM droplet sizes do not follow a linear tendency with the W_0 value, thus showing the considerable NaDEHP interdroplet interaction. Consequently, QB senses not only a less polar microenvironment but also less hydrogen-bond donor for the NaDEHP RM interface in comparison with the AOT/toluene media. Thus, upon confinement the water sequestrated in NaDEHP RMs seems to be more associated with other water molecules than with the surfactant polar head. This surprising result is completely different from those found for AOT RMs, in which the confinement makes the inter-

facial water (low W_0 value) less self-associated than the bulk water because of the strong water–AOT interaction.[1,6]

To gain more insights into these findings, we measured the O–H stretching frequency (ν_{OH}) for water encapsulated in both RMs and compared it with the corresponding water bulk value. At $W_0 = 1$ the ν_{OH} values obtained were 3495, 3368, and 3417 cm^{-1} for AOT/toluene, NaDEHP/toluene, and bulk water, respectively. Similar values were obtained at $W_0 = 1$ for AOT/*n*-heptane and NaDEHP/*n*-heptane systems by Li et al.[18,20] The fact that the ν_{OH} value is higher in AOT/toluene RMs than in bulk water confirms that the hydrogen-bond network present in pure water is destroyed upon encapsulation in AOT RMs, as is already known.[3,6,21] On the other hand, the ν_{OH} value is lower in the NaDEHP/toluene systems than in bulk water, thus suggesting that the water hydrogen bond is enhanced upon confinement by NaDEHP RMs. Perhaps the ellipsoidal form and the large size of NaDEHP at this low W_0 value[17] could be the cause of this interesting effect.

As is known, in bulk water the phosphate group (polar head of NaDEHP) is a stronger base than the sulfonate group (polar head of AOT) since phosphoric acid is weaker than sulfonic acid. Therefore, and contrary to our findings, the water–NaDEHP interaction could be expected to be stronger than the water–AOT interaction. Our results challenge this expectation because, as was demonstrated, acid–base equilibriums change dramatically at the RM interfaces due to the enormous ionic strength.[8,47] Moreover, we did not see the O–H stretching frequency of the nonionized phosphoric group at any W_0 values investigated.

Here, it is worth making a comparison between the K_p values for QB in both RMs (Table S1). It can be seen that 1) the toluene penetration into the NaDEHP interface, 2) the weak water–NaDEHP interaction, 3) the strong water–water interaction present in the NaDEHP RMs, and 4) the ellipsoidal and bigger NaDEHP RM size make the NaDEHP RM interface more fluid than that of the AOT RMs, which favors QB partition toward the RM pseudophase with a consequent higher K_p value than that obtained for the AOT RMs. Recently, we have demonstrated for other molecular probes that the fluidity of the AOT RM interfaces dramatically affects the partition process.[25]

PRODAN in Water/NaDEHP/Toluene RMs

Since QB seems to detect differences in the microviscosity between NaDEHP and AOT RM interfaces, we wanted to gain more insight by investigating the fluorophore PRODAN. In general, for a fluorophore in a bulk nonviscous solvent, the dipolar relaxation of the solvent molecules around it in the excited state is much faster than its fluorescence lifetime. Hence, the molecular probe photophysics is usually independent of the excitation wavelength. However, it does show excitation wavelength dependence if the dipolar relaxation of the solvent molecules is slow in the excited state, such that the relaxation time is comparable to or longer than the fluorescence lifetime. Fluorescence lifetime serves as a sensitive indicator for the local microenvironment where a solute exists, because the differential extent of solvent relaxation around a given fluorophore could be expected to give rise to differences in its fluorescence lifetime.[52–55] In motion-restricted media such as organized systems like RMs or vesicles, lifetimes are dependent on the excitation and emission wavelengths. Observation at shorter wavelengths of the emission spectra selects the unrelaxed fluorophores with shorter lifetimes, because this population decays both at the rate of fluorescence emission at the given excitation wavelength and at the rate of the emission at longer (unobserved) wavelengths. On the other hand, the observation at longer wavelengths (red edge) of the emission selects the more relaxed fluorophores, which have spent enough time in the excited state to allow a larger extent of solvent relaxation.[56] Thus, fluorescence lifetimes can be used to directly monitor the microenvironment and dynamics around a fluorophore in a motion-restricted environment, as was previously demonstrated for other molecular probes in RMs and vesicles.[53,54,56,57] Furthermore, PRODAN is a unique molecular probe since its emission state or states dramatically depend on the RM zone where PRODAN can be located.[25]

Figure 4 A–D show the PRODAN emission spectra obtained by varying the surfactant concentration at $W_0 = 1$ and 10 for NaDEHP/toluene RMs (Figure 4 A, C, respectively) and for AOT/toluene RMs (Figure 4 B, D, respectively). At $W_0 = 1$, in every system studied, as the surfactant concentration increases there is practically no variation in the maximum position of the absorption band (results not shown), whereas there is a slight (around 2 nm) bathochromic shift and a decrease of the intensity in the emission band (Figure 4 A, B). The situation is quite different at $W_0 = 10$, where the PRODAN behavior depends on the surfactant used to create the RMs. For NaDEHP (Figure 4 C) the trend is similar to the one described for $W_0 = 1$, whereas for AOT/toluene RMs (Figure 4 D) the results show that as the AOT concentration increases, there is a decrease in the intensity and a bathochromic shift of the band at $\lambda_{em} \approx 420$ nm (PRODAN in toluene) and also a new band emerges around 520 nm with an isoemissive point at $\lambda \approx 465$ nm.

The changes observed in Figure 4 show that the micropolarity of the environment sensed by PRODAN increases,[32] in comparison to that in toluene, due to the gradual incorporation of the molecule into the AOT and NaDEHP RM interfaces. Moreover, different emission maxima are observed at different excitation wavelengths (results not shown) due to the PRODAN heterogeneity in the ground state of the molecule.[58] Indeed, PRODAN emits from two different microenvironments: the organic nonpolar pseudophase and the RM interfaces. The K_p values calculated from the PRODAN emission spectral changes obtained by varying the surfactant concentration are gathered in Table S1 (Supporting Information).

Table 2 shows the fluorescence lifetimes for PRODAN in water/NaDEHP/toluene and water/AOT/toluene RMs at 0.01 M surfactant concentration and $W_0 = 1$ and 10. In both systems the decays were monitored at two emission wavelengths: $\lambda_{em} = 420$ and 500 nm. For AOT RMs at $W_0 = 10$ the pre-exponential factor is included for the band peaking at lower energy ($\lambda_{em} = 500$ nm).

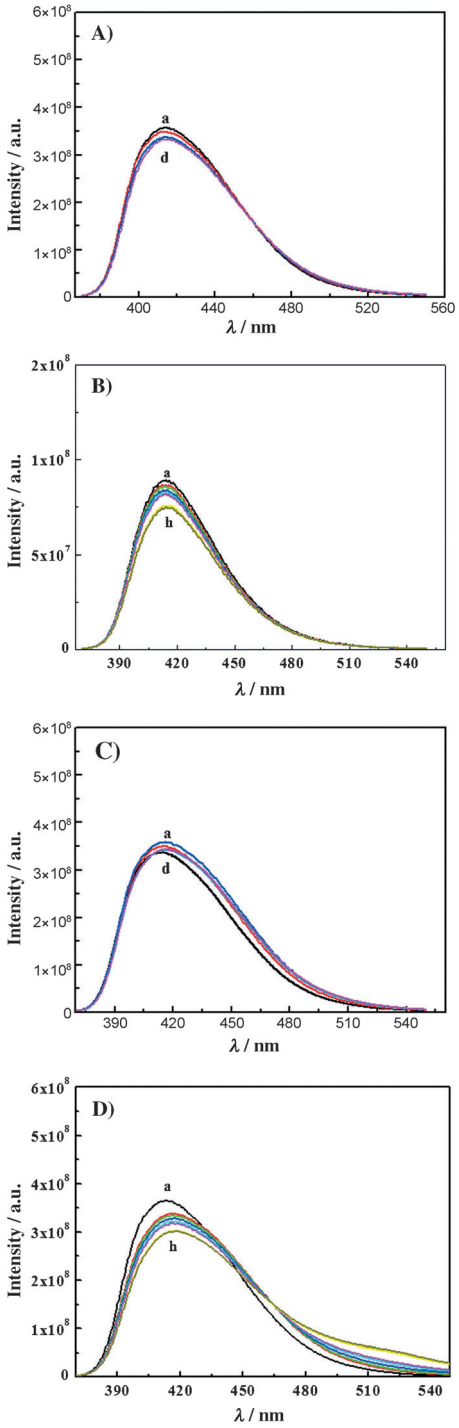

Figure 4. A) Emission spectra (λ_{exc}: 350 nm) of PRODAN with varying [NaDEHP] at $W_0=1$ in water/NaDEHP/toluene RMs. [NaDEHP]: a) 0, b) 8×10^{-3}, c) 2×10^{-2}, d) 0.2 M. [PRODAN] $=5\times10^{-6}$ M. B) Emission spectra (λ_{exc}: 350 nm) of PRODAN with varying [AOT] at $W_0=1$ in water/AOT/toluene RMs. [AOT]: a) 0, b) 8×10^{-3}, c) 2×10^{-2}, d) 5×10^{-2}, e) 8×10^{-2}, f) 0.1, g) 0.18, h) 0.2 M. [PRODAN] $=5\times10^{-6}$ M. C) Emission spectra (λ_{exc}: 350 nm) of PRODAN with varying [NaDEHP] at $W_0=10$ in water/NaDEHP/toluene RMs. [NaDEHP]: a) 0, b) 2.5×10^{-3}, c) 8×10^{-3}, d) 0.01 M. [PRODAN] $=5\times10^{-6}$ M. D) Emission spectra (λ_{exc}: 350 nm) of PRODAN with varying [AOT] at $W_0=10$ in water/AOT/toluene RMs. [AOT]: a) 0, b) 8×10^{-3}, c) 2×10^{-2}, d) 5×10^{-2}, e) 8×10^{-2}, f) 0.1, g) 0.18, h) 0.2 M. [PRODAN] $=5\times10^{-6}$ M.

Table 2. Fluorescence lifetimes (τ) of PRODAN in water/AOT/toluene and water/NaDEHP/toluene. [PRODAN] $=5\times10^{-6}$ M. [Surfactant] $=0.01$ M.

System	W_0	λ_{em}	τ_1 [ns] (%)[a]	τ_2 [ns] (%)[a]	χ^2
AOT/toluene	1	420	2.69 ± 0.04 (60)	1.90 ± 0.06 (40)	1.11
		500	–	2.62 ± 0.05	1.14
	10	420	2.68 ± 0.06 (20)	1.09 ± 0.04 (80)	1.08
		500	2.81 ± 0.06 (0.050)[b]	0.95 ± 0.04 (−0.052)[b]	1.09
NaDEHP/toluene	1	420	2.7 ± 0.2 (15)	1.3 ± 0.2 (85)	1.08
		500	–	1.85 ± 0.05	1.07
	10	420	2.56 ± 0.03 (26)	1.94 ± 0.09 (74)	1.14
		500	–	2.04 ± 0.04	1.14

[a] Values in parentheses are the contribution of the species obtained from the biexponential fitting. [b] Values in parentheses are the pre-exponential factor of the species obtained from the biexponential fitting.

In both systems at $W_0=1$ and at $\lambda_{em}=420$ nm, the fluorescence decay exhibits a biexponential decay with τ_1 close to the value that corresponds to PRODAN in toluene ($\tau=$ 2.42 ns).[24] Interestingly, the shorter component, τ_2, is emission wavelength dependent. On the other hand, in both RMs when monitoring at $\lambda_{em}=500$ nm the decays are monoexponential.

The PRODAN fluorescence lifetime values obtained in every system at $W_0=1$ and monitored at $\lambda_{em}=420$ nm (Table 2) confirm the partition process that PRODAN undergoes since two emission lifetimes are found. The longer component (τ_1) corresponds to the fluorescence lifetime of PRODAN in toluene, thus we assign the shorter component (τ_2) to the lifetime that corresponds to the probe in the NaDEHP and AOT RM interfaces. Since at $\lambda_{em}=500$ nm PRODAN in neat toluene does not emit, we only observe at this wavelength a monoexponential decay corresponding to the emission of the probe located at the RM interfaces (τ_2). Interestingly, τ_2 values are wavelength emission detection dependent, which means that PRODAN is located in motion-restricted media, the NaDEHP and AOT RM interfaces.[52] In addition, PRODAN emission from the AOT RM interface is much more dependent on the wavelength emission detection than from NaDEHP RM interface, which reveals the greater microviscosity that the AOT RM interface has in comparison with the NaDEHP RM interface.

Table S1 shows that the K_p value obtained at $W_0=1$ for the AOT reverse micellar media is smaller than that obtained for the NaDEHP RMs. As was previously found for QB, the partition process that PRODAN undergoes also shows the more structured and rigid AOT RM interface in comparison with NaDEHP RMs.

For NaDEHP/toluene RMs at $W_0=10$ and with monitoring at $\lambda_{em}=420$ nm the decays are also biexponential. At $\lambda_{em}=$ 500 nm the decay is monoexponential and the τ_2 value depends less on the emission wavelength in comparison with the system at low water content. Thus, at $W_0=10$ PRODAN still undergoes the partition process explained for $W_0=1$, and the two emission lifetimes observed in NaDEHP RMs at $\lambda_{em}=$ 420 nm can be assigned as follows: the longer component is PRODAN emission from toluene and the other component is PRODAN emission from the RM interface. Also note that τ_2 is

now practically independent of the wavelength emission detection, which reflects that PRODAN emits from a more fluid microenvironment when water is present in the NaDEHP RMs. Because the K_p value is smaller than the one at $W_0=1$ (Table S1), PRODAN is less incorporated into the RM pseudophase. Thus, we assume that PRODAN emits from the oil side of the NaDEHP RM interface. Therefore, the weak water–NaDEHP interaction and the toluene penetration toward the interface make the oil side of the RMs the more propitious site for PRODAN to reside. Moreover, PRODAN solubility in water is very low[25] and the molecular probe prefers a nonaqueous environment within the NaDEHP RMs.

For PRODAN in water/AOT/toluene RMs at $W_0=10$, the emission lifetime values shown in Table 2 at $\lambda_{em}=420$ nm show that PRODAN emits from toluene (τ_1) and from the RM interface (τ_2). A different situation is revealed when the longer emission wavelength, $\lambda_{em}=500$ nm, is analyzed. As can be seen, the fluorescence decays fit well to a double exponential function but the shorter component (τ_2) has a negative pre-exponential factor. A similar situation was previously found for PRODAN in aqueous and nonaqueous AOT/*n*-heptane RMs.[24,25] Moreover, the changes shown in Figure 4D evidence, in addition to the PRODAN partition process, the appearance of a new emerging band around 520 nm. A priori, the observation of negative amplitudes indicates that before the radiative de-excitation, a fast process compared to the emission lifetime exists, thus leading to an increase in the emitting population observed by fluorescence. In other words, there is an excited-state process leading to a new emitting state different from the initially excited state, which can explain the PRODAN dual fluorescence observed in the AOT RMs at $W_0=10$.[24,52] We attribute this process to a dual PRODAN emission from two different states: the LE state with emission band at λ_{max} around 420 nm and the ICT state with emission band at $\lambda_{max}=520$ nm. As is known,[24,36,37,52,59] PRODAN is a kind of molecule that is capable of simultaneously creating LE and ICT excited states. We have already demonstrated[24,25] that AOT and benzyl-*n*-hexadecyldimethylammonium chloride (BHDC) RM interfaces are unique environments for PRODAN to show the dual fluorescence process (i.e., emission from both states at the same time). Also, we have demonstrated that by changing the characteristics of the AOT RM interface, it is possible to switch the state or states from which PRODAN emits.[25] Now, PRODAN exhibits the dual fluorescence only from the AOT RM interface and not from the NaDEHP RM interface. Thus, it seems that the water–surfactant interactions play a key role in creating the unique environment that PRODAN needs to show the dual fluorescence. Perhaps the NaDEHP RM interface is not rigid enough to allow the molecular probe to undergo the dual fluorescence at any water content when PRODAN exists at this interface.

Interestingly, the K_p value obtained for PRODAN in the AOT RMs at $W_0=10$ is almost five times larger than that obtained at $W_0=1$, a result that can be explained by considering that, apart from the partition process, K_p also includes the ICT process that PRODAN undergoes in this AOT RM.

3. Conclusions

We have investigated two different reverse micellar interfaces, water/NaDEHP/toluene and water/AOT/toluene, at two water contents by using the solvatochromism behavior of two molecular probes: QB and PRODAN. We chose these molecular probes because they are sensitive to different medium effects and very valuable information on the reverse micellar media can be obtained.

Our results demonstrate that because of the water–NaDEHP interaction the interfacial properties of NaDEHP RMs are very peculiar and different from those found for AOT RMs. The interfacial water structure inside NaDEHP RMs has the water–water hydrogen-bond interaction enhanced in comparison with bulk water. The aromatic nonpolar solvent penetration into the NaDEHP interface offers a medium with lower micropolarity and microviscosity than those of AOT. These findings show that the NaDEHP RM interface properties are not comparable to the well-known properties of the AOT RM interface, where the strong water–AOT interaction makes the interface rigid, with high micropolarity and with an interfacial water structure with the hydrogen-bond network destroyed upon encapsulation.[3,6,21,57]

In summary, the work shows how the properties of different reverse micellar interfaces can be dramatically changed simply by using different anionic surfactants. This result can be very useful to employ RMs as nanoreactors.

Experimental Section

Materials: 1-Methyl-8-oxyquinolinium betaine (QB) was synthesized by a procedure reported previously.[45] The fluorescent probe 6-propionyl-2-(*N*,*N*-dimethyl)aminonaphthalene (PRODAN) from Molecular Probes (Eugene, OR) was used without further purification. Sodium 1,4-bis(2-ethylhexyl) sulfosuccinate (AOT) from Sigma Aldrich (>99% purity) was used as received. Sodium bis(2-ethylhexyl) phosphate (NaDEHP) was synthesized according ref. [60]. Both surfactants were kept under vacuum over P_2O_5 to minimize H_2O absorption. The absence of acidic impurities was confirmed through the QB absorption bands.[21] Toluene and benzene (Merck spectroscopic quality) were used as received and ultrapure water was obtained from Labonco equipment model 90901-01.

Methods: Stock solutions of AOT and NaDEHP in the aromatic solvents were prepared by mass and volumetric dilution. To obtain optically clear solutions they were shaken in a sonicating bath and water was added using a calibrated microsyringe. The amount of water present in the system is expressed as the molar ratio between polar solvent and the surfactant (W_0=[water]/[surfactant]) and was kept constant and equal to 1 or 10 in every system investigated.

To introduce the molecular probes, a 0.01 M solution of QB (or PRODAN) was prepared in methanol (or acetonitrile) (Sintorgan, HPLC quality). The appropriate amount of this solution to obtain a given concentration (2×10^{-4} M for QB and 5×10^{-6} M for PRODAN) of the probe in the micellar medium was transferred into a volumetric flask, and the methanol (or acetonitrile) was evaporated by bubbling dry N_2; then, the surfactant RM solution was added to the residue to obtain a [surfactant]=0.2 M. The stock solution of surfactant (0.2 M) and the molecular probe were agitated in a soni-

cating bath until the microemulsion was optically clear. Appropriate amounts of surfactant and molecular probe stock solution were added to a cell bearing QB (or PRODAN, 2 mL) of the same concentration in the aromatic solvent, to obtain a given concentration of surfactant in the micellar media. Therefore, the absorption or emission of the molecular probe was not affected by dilution.

General: UV/Vis spectra were recorded using a Shimadzu 2401 spectrophotometer with a thermostated sample holder. A Spex fluoromax apparatus was employed for the fluorescence measurements. Corrected fluorescence spectra were obtained using the correction file provided by the manufacturer. The path length used in the absorption and emission experiments was 1 cm. λ_{max} was measured by taking the midpoint between the two positions of the spectrum where the absorbance is equal to $0.9 \times A_{max}$. The uncertainties in λ_{max} were about 0.1 nm.

Fluorescence decay data were measured with the time-correlated single photon counting technique (Edinburgh Instruments FL-900) with a PicoQuant sub-nanosecond pulsed LED PLS 375 apparatus (emitting at 375 nm), $<$ 600 ps full width at half maximum (FWHM), collecting a total of 10 000 counts. Fluctuations in the pulse and intensity were corrected by making an alternate collection of scattering and sample emission. The choice between a single or a double exponential fit was made on the basis of the presence or absence of any observed deviation from random fluctuation in residual plots and the values of the chi-squared parameter (χ^2).[61] For the best fit χ^2 must be around 1.0–1.2.[62] It should be noted that in the case of the single exponential fit we tried to perform multiexponential fitting but the statistics of the decays were not improved at all, or sometimes they became worse.

FTIR spectra were recorded with a Nicolet IMPACT 400 FTIR spectrometer. IR cells of the type Irtran-2 (0.5 mm path length) from Wilmad Glass (Buena, NJ) were used. FTIR spectra were obtained by co-adding 200 spectra at a resolution of 0.5 cm^{-1}, and the aromatic solvent spectrum was used as the background.

Acknowledgements

We gratefully acknowledge the financial support for this work by the Consejo Nacional de Investigaciones Científicas y Técnicas (CONICET), Agencia Córdoba Ciencia, Agencia Nacional de Promoción Científica y Técnica, and Secretaría de Ciencia y Técnica de la Universidad Nacional de Río Cuarto. N.M.C., J.J.S. and R.D.F. hold research positions at CONICET. S.S.Q. thanks CONICET for a research fellowship.

Keywords: molecular probes · interfaces · reverse micelles · solvatochromism · surfactants

[1] a) S. P. Moulik, *Curr. Sci.* **1996**, *71*, 368; b) S. P. Moulik, B. K. Paul, *Adv. Colloid Interface Sci.* **1998**, *78*, 99.
[2] V. Uskoković, M. Drofenik, *Adv. Colloid Interface Sci.* **2007**, *133*, 23.
[3] K. De, A. Maitra, *Adv. Colloid Interface Sci.* **1995**, *59*, 95.
[4] M. A. Biasutti, N. M. Correa, J. J. Silber, *Curr. Top. Colloid Interface Sci.* **1999**, *3*, 35.
[5] A. Yehta, M. Aikawa, N. Turro, *J. Chem. Phys. Lett.* **1979**, *63*, 543.
[6] J. J. Silber, A. Biasutti, E. Abuin, E. Lissi, *Adv. Colloid Interface Sci.* **1999**, *82*, 189.
[7] D. Grand, A. Dokutchaev, *J. Phys. Chem. B* **1997**, *101*, 3181.
[8] B. B. Raju, S. M. B. Costa, *J. Phys. Chem. B* **1999**, *103*, 4309.
[9] L. C. Dong, S. J. Huang, Q. Luo, X. H. Zhou, S. S. Zheng, *Biochem. Eng. J.* **2009**, *46*, 210.
[10] a) H. F. Eicke, H. Christen, *J. Colloid Interface Sci.* **1974**, *46*, 417; b) H. F. Eicke, H. Christen, *J. Colloid Interface Sci.* **1974**, *48*, 281.
[11] A. Faure, A. M. Tistchenko, T. Zemb, C. Chachaty, *J. Phys. Chem.* **1985**, *89*, 3373.
[12] A. Faure, T. Ahlnas, A. M. Tistchenko, C. Chachaty, *J. Phys. Chem.* **1987**, *91*, 1827.
[13] Z. J. Yu, N. F. Zhou, R. D. Neuman, *Langmuir* **1992**, *8*, 1885.
[14] a) Z. J. Yu, R. D. Neuman, *Langmuir* **1994**, *10*, 2553; b) Z. J. Yu, R. D. Neuman, *J. Am. Chem. Soc.* **1994**, *116*, 4075.
[15] Z. J. Yu, R. D. Neuman, *Langmuir* **1995**, *11*, 1081.
[16] T. H. Ibrahim, *J. Franklin Inst.* **2010**, *347*, 875.
[17] a) K. I. Feng, Z. A. Schelly, *J. Phys. Chem.* **1995**, *99*, 17207; b) K. I. Feng, Z. A. Schelly, *J. Phys. Chem.* **1995**, *99*, 17212.
[18] Q. Li, S. Weng, J. Wu, H. Zhou, *J. Phys. Chem. B* **1998**, *102*, 3168.
[19] Q. Li, J. Wu, N. Zhou, *J. Colloid Interface Sci.* **2000**, *229*, 298.
[20] Q. Li, T. Li, J. Wu, *J. Phys. Chem. B* **2000**, *104*, 9011.
[21] N. M. Correa, M. A. Biasutti, J. J. Silber, *J. Colloid Interface Sci.* **1995**, *172*, 71.
[22] N. M. Correa, M. A. Biasutti, J. J. Silber, *J. Colloid Interface Sci.* **1996**, *184*, 570.
[23] R. D. Falcone, N. M. Correa, M. A. Biasutti, J. J. Silber, *Langmuir* **2000**, *16*, 3070.
[24] M. Novaira, M. A. Biasutti, J. J. Silber, N. M. Correa, *J. Phys. Chem. B* **2007**, *111*, 748.
[25] M. Novaira, F. Moyano, M. A. Biasutti, J. J. Silber, N. M. Correa, *Langmuir* **2008**, *24*, 4637.
[26] B. Sengupta, J. Guharay, P. K. Sengupta, *Spectrochim. Acta Part A* **2000**, *56*, 1433.
[27] K. K. Karukstis, A. A. Frazier, D. S. Martula, J. A. Whiles, *J. Phys. Chem.* **1996**, *100*, 11133.
[28] K. K. Karukstis, A. A. Frazier, C. T. Loftus, A. S. Tuan, *J. Phys. Chem. B* **1998**, *102*, 8163.
[29] E. A. Lissi, E. B. Abuin, M. A. Rubio, A. Cerón, *Langmuir* **2000**, *16*, 178.
[30] K. K. Karukstis, C. A. Zieleniuk, M. J. Fox, *Langmuir* **2003**, *19*, 10054.
[31] G. Weber, F. J. Farris, *Biochemistry* **1979**, *18*, 3075.
[32] F. Moyano, M. A. Biasutti, J. J. Silber, N. M. Correa, *J. Phys. Chem. B* **2006**, *110*, 11838.
[33] E. K. Krasnowska, E. Gratton, T. Parasassi, *Biophys. J.* **1998**, *74*, 1984.
[34] T. Parasassi, E. K. Krasnowska, L. A. Bagatolli, E. Gratton, *J. Fluoresc.* **1998**, *8*, 365.
[35] E. K. Krasnowska, L. A. Bagatolli, E. Gratton, T. Parasassi, *Biochim. Biophys. Acta Biomembr.* **2001**, *1511*, 330.
[36] Z. R. Grabowski, K. Rotkiewicz, W. Rettig, *Chem. Rev.* **2003**, *103*, 3899.
[37] A. Balter, W. Nowak, W. Pawelkiewicz, A. Kowalczyk, *Chem. Phys. Lett.* **1988**, *143*, 565.
[38] J. Catalan, P. Perez, J. Laynez, F. G. Blanco, *J. Fluoresc.* **1991**, *1*, 215.
[39] F. Moreno, S. Corrales, P. Sevilla, F. G. Blanco, C. Diaz, J. Catalán, *Helv. Chim. Acta* **2001**, *84*, 3306.
[40] R. Adhikary, C. A. Barnes, J. W. Petrich, *J. Phys. Chem. B* **2009**, *113*, 11999.
[41] N. M. Correa, J. J. Silber, *J. Mol. Liq.* **1997**, *72*, 163.
[42] N. M. Correa, E. N. Durantini, J. J. Silber, *J. Colloid Interface Sci.* **1998**, *208*, 96.
[43] N. M. Correa, E. N. Durantini, J. J. Silber, *J. Colloid Interface Sci.* **2001**, *240*, 573.
[44] L. Zingaretti, N. M. Correa, L. Boscatto, S. M. Chiacchiera, E. N. Durantini, S. G. Bertolotti, C. R. Rivarola, J. J. Silber, *J. Colloid Interface Sci.* **2005**, *286*, 245.
[45] M. Ueda, Z. A. Schelly, *Langmuir* **1989**, *5*, 1005.
[46] R. D. Falcone, N. M. Correa, J. J. Silber, *Langmuir* **2009**, *25*, 10426.
[47] F. M. Menger, G. Saito, *J. Am. Chem. Soc.* **1978**, *100*, 4376.
[48] H. C. Hung, G. G. Chang, *J. Chem. Soc. Perkin Trans. 2* **1999**, 2177.
[49] N. M. Correa, E. N. Durantini, J. J. Silber, *J. Org. Chem.* **2000**, *65*, 6427.
[50] N. M. Correa, E. N. Durantini, J. J. Silber, *J. Org. Chem.* **1999**, *64*, 5757.
[51] B. Baruah, J. M. Roden, M. Sedgwich, N. M. Correa, D. C. Crans, N. E. Levinger, *J. Am. Chem. Soc.* **2006**, *128*, 12758.
[52] J. R. Lakowicz in *Principles of Fluorescence Spectroscopy, 2nd ed.*, Kluwer Academic, New York, **1999**.
[53] A. Chattopadhyay, S. Murkherjee, H. Raghuraman, *J. Phys. Chem. B* **2002**, *106*, 13002.
[54] F. M. Moyano, J. J. Silber, N. M. Correa, *J. Colloid Interface Sci.* **2008**, *317*, 332.

[55] J. Kim, M. Lee, *J. Phys. Chem. A* **1999**, *103*, 3378.
[56] A. Chattopadhyay, *Chem. Phys. Lipids* **2003**, *122*, 3.
[57] F. Moyano, S. S. Quintana, R. D. Falcone, J. J. Silber, N. M. Correa, *J. Phys. Chem. B* **2009**, *113*, 4284.
[58] R. D. Falcone, N. M. Correa, M. A. Biasutti, J. J. Silber, *J. Colloid Interface Sci.* **2006**, *296*, 356.
[59] A. Balter, W. Nowak, W. Pawelkiewicz, A. Kowalczyk, *Chem. Phys. Lett.* **1988**, *143*, 565.
[60] A. Ruggirello, V. T. Liveri, *J. Colloid Interface Sci.* **2003**, *258*, 123.
[61] T. H. N. Pham, R. J. Clarke, *J. Phys. Chem. B* **2008**, *112*, 6513.
[62] D. V. O'Connor, D. Phillips, *Time-Correlated Single Photon Counting, Chapter 6*, Academic Press, New York, **1983**.

Received: August 20, 2011
Revised: October 21, 2011
Published online on December 1, 2011

